

# The Reynolds number effect on dynamics of the wake behind a circular cylinder

Cite as: AIP Conference Proceedings **2189**, 020023 (2019); <https://doi.org/10.1063/1.5138635>  
Published Online: 22 November 2019

Václav Uruba, and Pavel Procházka



View Online



Export Citation

## ARTICLES YOU MAY BE INTERESTED IN

[An experimental research of the DSPW steam turbine control valve](#)

AIP Conference Proceedings **2189**, 020012 (2019); <https://doi.org/10.1063/1.5138624>

[Testing of the seismic response in software ANSYS](#)

AIP Conference Proceedings **2189**, 020019 (2019); <https://doi.org/10.1063/1.5138631>

[Theoretical problems of calculation methods of turbulent flows](#)

AIP Conference Proceedings **2189**, 020025 (2019); <https://doi.org/10.1063/1.5138637>



## Your Qubits. Measured.

Meet the next generation of quantum analyzers

- Readout for up to 64 qubits
- Operation at up to 8.5 GHz, mixer-calibration-free
- Signal optimization with minimal latency

Find out more



# The Reynolds Number Effect on Dynamics of the Wake behind a Circular Cylinder

Václav Uruba<sup>1, 2, a)</sup> and Pavel Procházka<sup>1, b)</sup>

<sup>1</sup>*Institute of Thermomechanics of the Czech Academy of Sciences, Dolejškova 5, 182 00 Praha 8, Czech Republic*

<sup>2</sup>*University of West Bohemia, Faculty of Mechanical Engineering, Department of Power System Engineering, Univerzitní 8, Plzeň, Czech Republic*

<sup>a)</sup>Corresponding author: uruba@it.cas.cz

<sup>b)</sup>prochap@it.cas.cz

**Abstract.** Circular cylinder in cross-flow was studied experimentally using time-resolved PIV technique. Reynolds numbers based on the cylinder diameter were in range from 3 850 up to 19 260. Effect of the Reynolds number on wake time-mean topology as well as the dynamical behavior is studied. The wake dynamics is analyzed using the OPD method. The Oscillation Pattern Decomposition method provides unique information on dynamical patterns topology and oscillations in the flow-field. The pseudo-periodical wavy patterns have been detected within the cylinder wake. The parameters of this behavior are Reynolds number dependent, especially their sizes and shapes. Typical flow-field topologies are presented in the paper. The study is of qualitative character as flow boundary conditions are not well defined.

## INTRODUCTION

Circular cylinder in cross-flow is one of the canonical cases representing flow around a bluff-body. This case is addressed in numerous studies, experimental, theoretical and CFD. It is known, that for Reynolds numbers higher than about 44 the von Karman vortex street exists, which exhibits typical dynamics of the wake.

Two dimensionless parameters characterize the wake dynamics. The Reynolds number  $Re$  is dimensionless velocity and the Strouhal number  $St$  is dimensionless frequency:

$$Re = \frac{U \cdot D}{\nu}, \quad St = \frac{f \cdot D}{U}, \quad (1)$$

where  $U$  is the incoming flow velocity,  $D$  is the cylinder diameter,  $\nu$  is the kinematic viscosity of the fluid and  $f$  is the shedding frequency of vortices in wake. The dependence of  $St$  on  $Re$  is shown in graph in Figure 1. The graph was published in [2], uses data from [1,3,6].

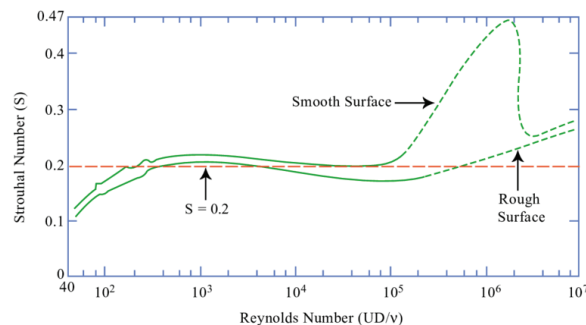


FIGURE 1. Strouhal number for circular cylinder [2].

The presented experiments will show results for Reynolds numbers 3 850, 4 815, 9 630 and 19 260 respectively, the corresponding Strouhal number from graph in figure 1 is about 0.2.

## EXPERIMENTAL SETUP

The cylinder of diameter 15 mm is placed perpendicularly to the flow issuing from the blown-down facility exit. The test section is open, the flow forms a free jet. The cross-section of the free jet is 250 x 250 mm<sup>2</sup> in the position of the cylinder, the cylinder length is 300 mm.

The velocity vector field was measured using Particle Image Velocimetry (PIV) method. The measurement apparatus consists of laser and CMOS camera by Dantec company. The laser is New Wave Pegasus, Nd:YLF double head with wavelength of 527 nm, maximal frequency 10 kHz, shot energy is 10 mJ (for 1 kHz) and corresponding power is 10 W per one head. The camera Phantom V611 with resolution of 1 280 x 800 pixels is able to acquire double snaps with frequency up to 3000 Hz (full resolution) and it uses internal memory 8 GB. The data were acquired and post-processed in Dynamic Studio and Matlab software.

The PIV measurement was performed in the plane perpendicular to the cylinder axis and parallel to the flow direction ( $xy$ ). The evaluated velocity fields consisting of 159 x 99 vectors were acquired in two different regimes. Statistics were evaluated from data acquired with frequency 100 Hz, 2 000 double-snapshots representing 20 s in real time. The dynamical analysis was performed on data acquired by frequency 2 kHz, one record contained 4 000 double-snapshots representing 2 s in real time. More detailed description of the experimental setup could be found in [4].

## RESULTS

All results are to be shown in dimensionless form. The geometric dimensions are expressed in multiples of the cylinder diameter  $D$  and the velocities in multiples of the inlet velocity  $U$ .

The Cartesian coordinate system has origin in the center of the cylinder,  $x$  axis is oriented in the flow direction, while the  $y$  axis is perpendicular to the flow direction and the cylinder axis. The Reynolds number value is to be shown in upper left corner for each result.

Two types of results are to be presented. First, distributions of statistical quantities are to be shown, next dynamical analysis is presented obtained using the OPD method.

### Time-Mean Statistics

In Figure 2 there is mean velocity vectors distribution. The vector-lines are added to recognize better the flow-field structure.

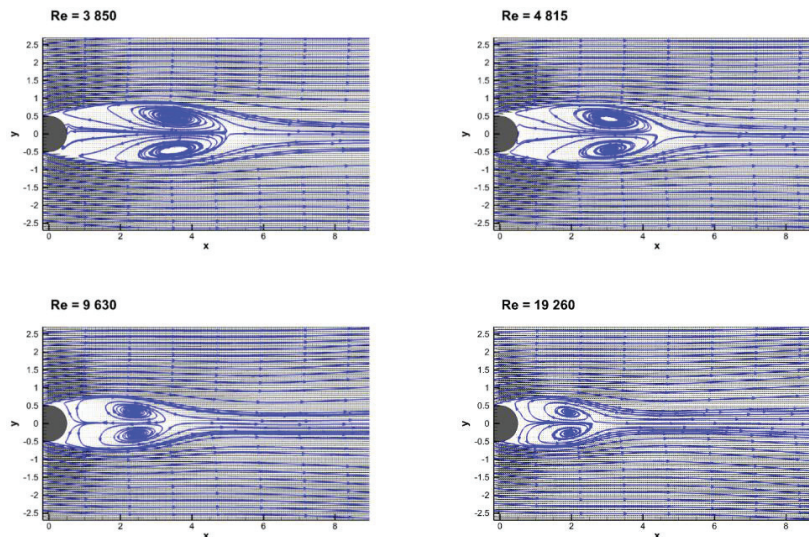
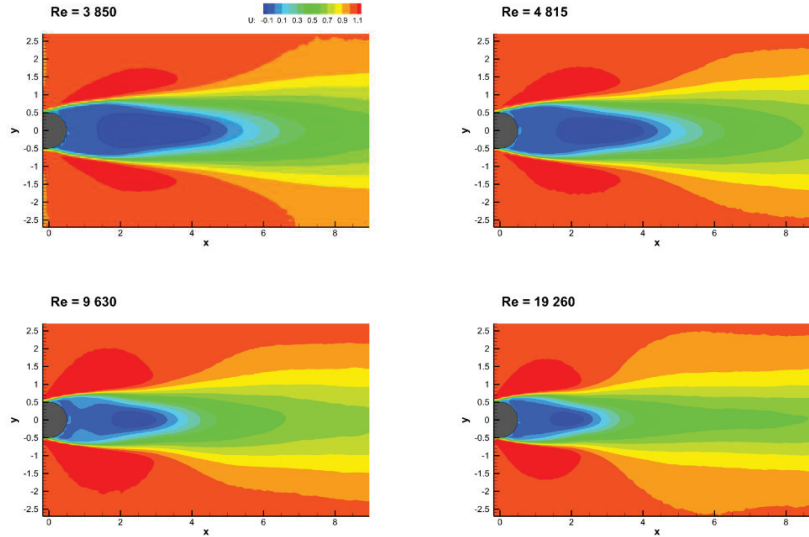


FIGURE 2. Vector-lines of the mean velocity vector fields.

The mean-flow wake is located behind the cylinder forming two counter-rotating vortices located symmetrically. The sizes and positions of the vortices are Reynolds number dependent. Positions of the mean-flow vortices centers in  $x$  are approximately 3.5, 3, 2.5 and 2 respectively for ascending Re.

In Figure 3 the dimensionless streamwise mean velocity distributions are shown. Please note dark blue for back-flow, value of 1 (in red) means the same velocity as in the inlet.



**FIGURE 3.** Dimensionless mean streamwise velocity component  $U$  distributions.

The size of the back-flow region decreases with the Reynolds number value. Velocity overshoot is located on both sides of the wake just behind the cylinder.

The dimensionless Turbulence Kinetic Energy (TKE) is evaluated from the in-plane velocity fluctuations:

$$TKE = \frac{3}{4} \left( \overline{u'^2} + \overline{v'^2} \right), \quad (2)$$

where  $u'$  is the dimensionless streamwise velocity fluctuation,  $v'$  is the dimensionless spanwise velocity fluctuation and  $\overline{\quad}$  is the averaging operation. The incoming velocity is used as a reference. This formula is used instead of the classical formula defined as a half of sum of all 3 velocity component variances, as in our case the velocity in  $z$  direction in the cylinder axis direction is not measured. The given definition of the TKE quantifies the ratio of the local fluctuating kinetic energy and the kinetic energy of the incoming flow and thus it is dimensionless. Distributions of the TKE for individual Reynolds numbers are shown in Figure 4.

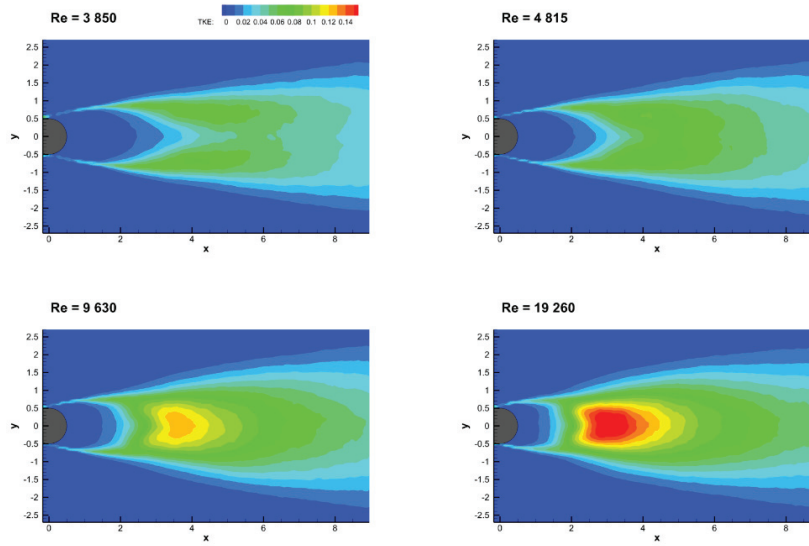


FIGURE 4. Dimensionless turbulent kinetic energy TKE distributions.

In the near wake very low fluctuating activity has been detected, the same as outside the wake (dark blue). The two regions of moderate TKE regions 0.05-0.1 (green) are located on sides of the middle wake  $x$  between 2 and 8. For higher Re 9 630 and 19 260 the other absolute maximum of the TKE is located on the axis  $y = 0$  in the distance of about  $x = 3.5$ . The maximum TKE is about 0.12 for Re = 9 630 and 0.15 for Re = 19 260.

The correlation coefficient  $r$  is dimensionless from its definition, it is defined within the interval  $\langle -1;1 \rangle$ .

$$r = \frac{\overline{u'v'}}{\sqrt{\overline{u'^2}}\sqrt{\overline{v'^2}}} \quad (3)$$

It could be linked to the Reynolds stress component. The correlation coefficient close to zero means negligible Reynolds stress and no turbulence production, as Reynolds stress value is decisive for the turbulence production term. The correlation coefficient close to  $+1$  means high turbulence production in the given spot. Distributions of the correlation coefficient in the cylinder wake are shown in Figure 5 for the Reynolds numbers in question.

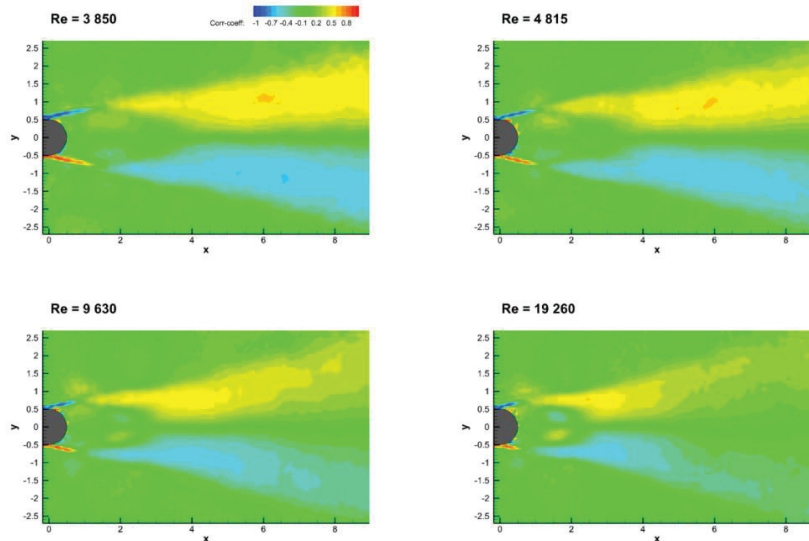


FIGURE 5. Correlation coefficient distributions.

The Figure 5 suggests high turbulence generation rate within the free shear layers emerging due to boundary layers separation. These regions are very thin, however the turbulence production process is of high intensity. Two bigger turbulence production regions are located in the wake symmetrically, the size of those regions is in inverse proportion to the Reynolds number. Maximum of the correlation coefficient within the wake is located in the distance  $x = 6$  for the  $Re = 3\,850$  and moves upstream, reaching position  $x = 3$  for the  $Re = 19\,260$ .

## Flow Dynamics

To study the dynamical properties of the flow-field the Oscillation Pattern Decomposition method (OPD) was adopted resulting in series of OPD modes. Each OPD mode is characterized by its topology in complex form (consisting of real and imaginary parts), frequency and attenuation of the pseudo-periodic (oscillating) behavior. Attenuation or amplitude decay is described by so called e-folding time representing mean time period of the mode amplitude decay by “e”. The other decay characteristic is “periodicity” which expresses the e-folding time in multiples of periods. The details on OPD method could be found in [7,9].

The OPD modes have been evaluated for all  $Re$ , they are depicted in the Strouhal number – Periodicity space in Figure 6. The number in the point represents number of the OPD mode ordered according to the periodicity value, the color is related to the Reynolds number. Up to ten modes have been evaluated for each Reynolds number.

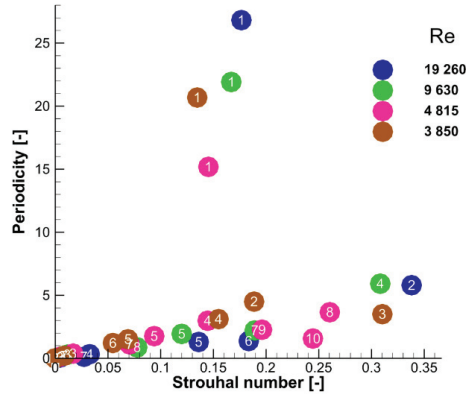


FIGURE 6. OPD modes in Periodicity – Strouhal number space for different Reynolds numbers.

The most important modes No. 1 for each Reynolds number represent dominant periodical process – the von Kármán Vortex Street.

In Table 1 parameters of the presented OPD modes are given in numerical form, only OPD modes 1 are given for all  $Re$ , the higher order modes are shown only for the  $Re = 4\,815$ . The Strouhal number  $St$  is calculated from the frequency  $f$  using the formula (1).

**TABLE 1.** Parameters of the presented OPD modes

Re	No	$f$ [Hz]	St [1]	$\tau_e$ [ms]	$p$ [1]
3 850	1	35.94	0.1348	575	20.68
4 815	1	48.44	0.1453	313	15.18
9 630	1	111.3	0.1670	197	21.91
19 260	1	235.4	0.1766	114	26.82
4 815	2	1.970	0.0059	75	0.149
4 815	3	5.663	0.0170	66	0.373
4 815	4	48.19	0.1446	62	2.978
4 815	5	31.31	0.0939	56	1.753
4 815	6	0	0	55	0
4 815	7	23.55	0.0706	47	1.105
4 815	8	86.85	0.2606	42	3.659
4 815	9	65.40	0.1962	35	2.264
4 815	10	81.50	0.2445	19	1.566

Topology of the selected modes is to be shown next. Each mode topology consists of real and imaginary parts respectively. The real part corresponds to the phase angle 0 of the process, while the imaginary part corresponds to the phase angle  $\pi/2$ , than phase  $\pi$  is characterized by negative real part and  $3\pi/2$  by negative imaginary part. The process is pseudo-periodical with decaying amplitude.

Topology is shown as vector fields. For a better clarity the vector-lines are added arbitrarily, for the real part in red and for the imaginary part in blue colours. Thus the vortical structures are visualised as closed or spiral lines.

First, the dominant OPD modes No. 1 for all Reynolds numbers are shown in Figures 7,8,9 and 10, respectively.

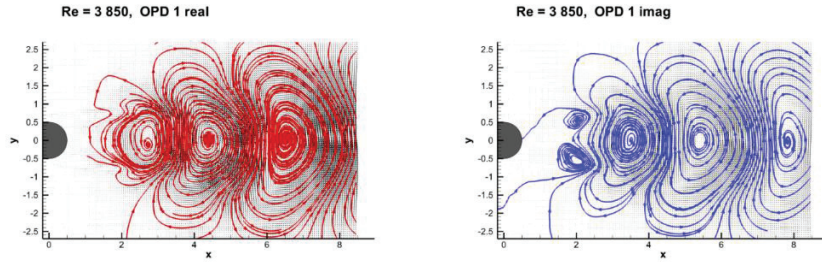


**FIGURE 7.** The OPD mode No. 1 topology, Reynolds number 3 850, real (left) and imaginary (right) parts.

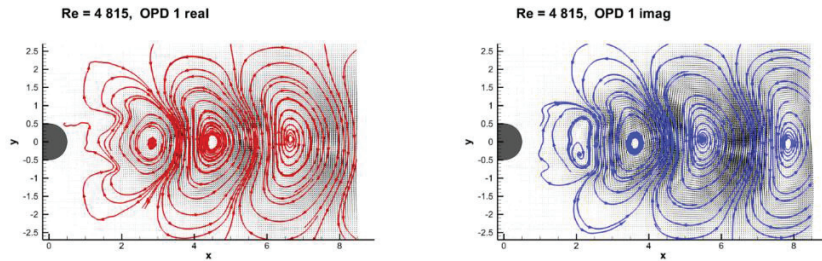


**FIGURE 8.** The OPD mode No. 1 topology, Reynolds number 4 815, real (left) and imaginary (right) parts.

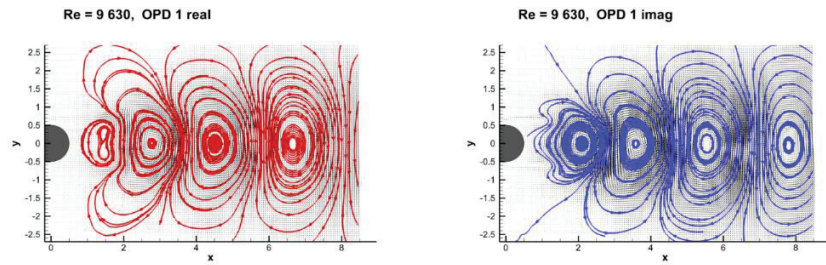


FIGURE 9. The OPD mode No. 1 topology, Reynolds number 9 630, real (left) and imaginary (right) parts.

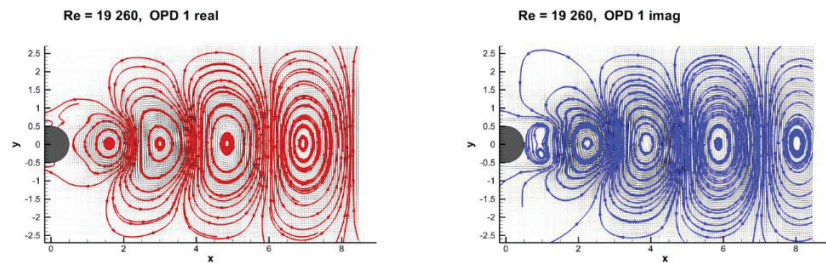


FIGURE 10. The OPD mode No. 1 topology, Reynolds number 19 260, real (left) and imaginary (right) parts.

All cases of dominant dynamical structure indicate the train of vortices with alternate orientation localized on the axis of symmetry  $x$ . The difference is in spacing of vortical structure, which is inversely related to the Reynolds number value.

The frequency and Strouhal number is about 25 % lower than expected. This could be the effect of the free jet, or more precisely presence of shear layers on the jet borders.

As the process is periodical with a given frequency, see Table 1, the velocity of vortices could be estimated from the structures spacing. The velocity of vortices is about 30 % of the inlet velocity  $U$  for all Reynolds numbers.

The process of the vortices formation could be studied from the real and imaginary parts topologies. The vortex origin is located in the near wake very close to the cylinder. In the region  $x < 2$  the two symmetrical vortices with the same orientation are present. Close to the position  $x = 2$  the two vortices merge into a single one located on the  $x$  axis. Localization of this process is slightly shifted to smaller distances for higher Reynolds numbers.

The higher order modes are to be shown next. As the topology of OPD modes is similar for all Reynolds numbers, results for only one Reynolds number  $Re = 4\ 815$  will be shown.

The OPD modes parameters are given in Table 1. The modes could be divided into decaying for  $p = 0$ , pulsatile ( $0 < p < 0.34$ ) and travelling waves ( $p > 0.34$ ). More details could be found in [7,9]. For the case of  $Re = 4\ 815$ , the mode 2 is pulsatile, the mode 6 is decaying and the other modes (1,3,4,5,7,8,9,10) represent travelling structures. The mode 1 is the dominant one with very high value of the periodicity  $p$  indicating relatively stable periodical behavior.

The OPD mode 2 in Figure 11 is characterized by very low frequency about 2 Hz, the topologies of real and imaginary parts are very similar to each other as for positions of vortical structure.

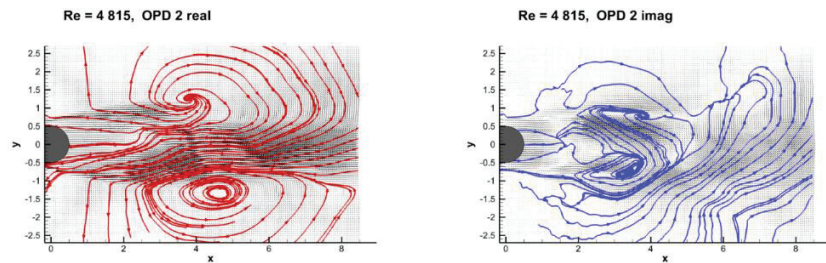


FIGURE 11. The OPD mode 2 topology, Reynolds number 4 815, real (left) and imaginary (right) parts.

The OPD mode 3 forms a jet in the wake region, see Figure 12.

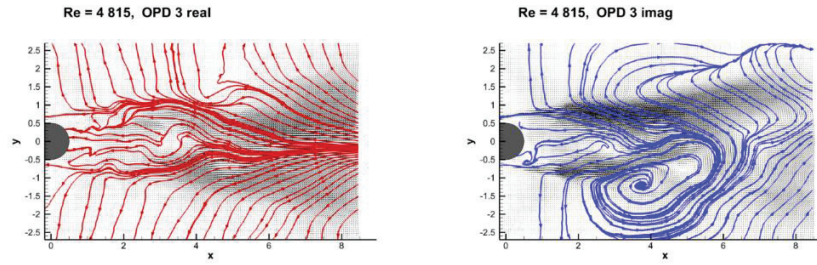


FIGURE 12. The OPD mode 3 topology, Reynolds number 4 815, real (left) and imaginary (right) parts.

Topology of the OPD mode 4 is similar to that of the mode 1, the frequencies are very close to each other. The mode 4 represents kind of minority deformation of the dominant mode 1, see Figure 13

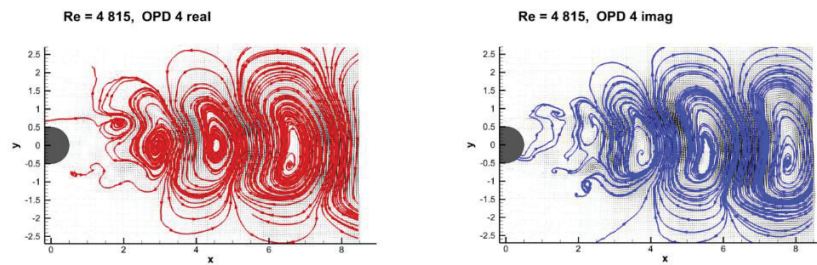


FIGURE 13. The OPD mode 4 topology, Reynolds number 4 815, real (left) and imaginary (right) parts.

The OPD modes 5, 6 and 7 in Figures 14, 15 and 16 are characterized by disordered structures consisting of a few solitary vortices. As the mode 6 is characterized by the frequency 0Hz, its imaginary part vanishes.

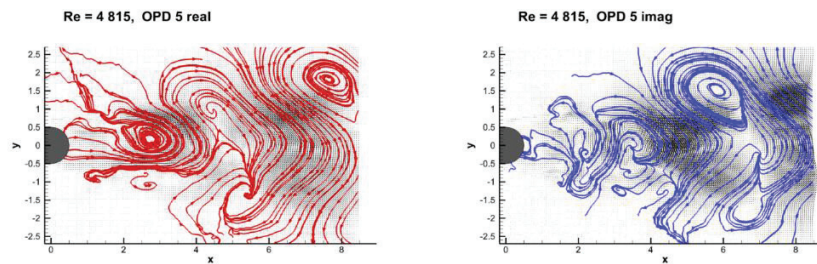


FIGURE 14. The OPD mode 5 topology, Reynolds number 4 815, real (left) and imaginary (right) parts.

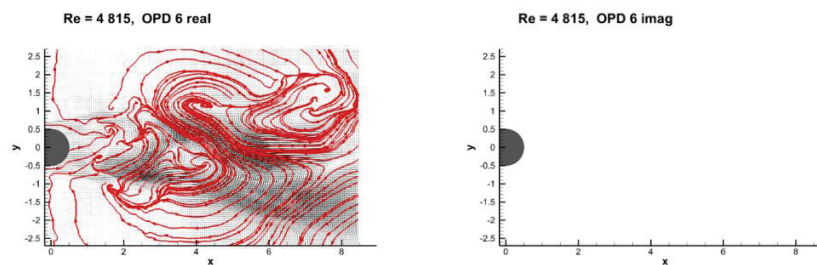


FIGURE 15. The OPD mode 6 topology, Reynolds number 4 815, real (left) and imaginary (right) parts.

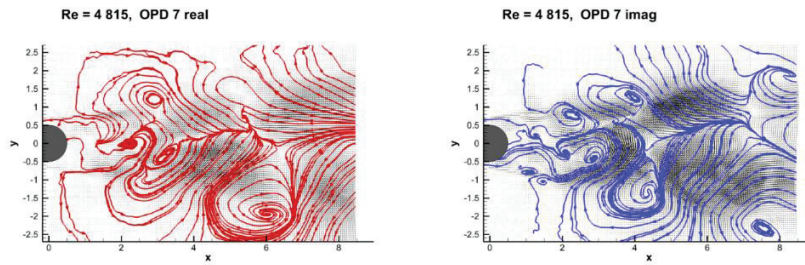


FIGURE 16. The OPD mode 7 topology, Reynolds number 4 815, real (left) and imaginary (right) parts.

The topologies of OPD modes 8, 9, 10 in Figures 17, 18 and 19 are represented by the vortex couples trains within the wakes, moving downstream. However the vortices in couples are oriented oppositely in the modes 8 and 10 forming the contra-rotating pairs, while in the mode 9 the vortices in couples are of identical orientation, changing it in the next row.

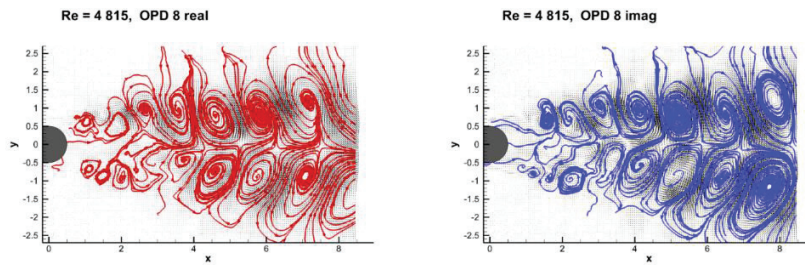


FIGURE 17. The OPD mode 8 topology, Reynolds number 4 815, real (left) and imaginary (right) parts.

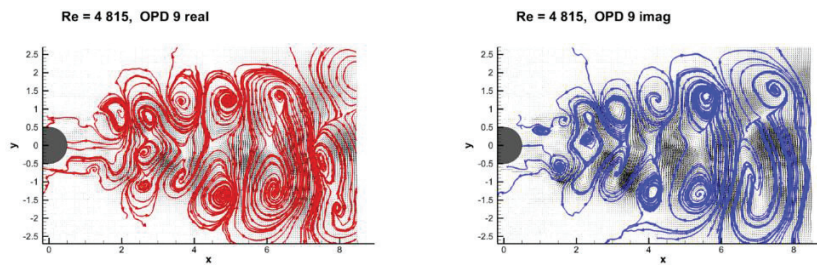


FIGURE 18. The OPD mode 9 topology, Reynolds number 4 815, real (left) and imaginary (right) parts.

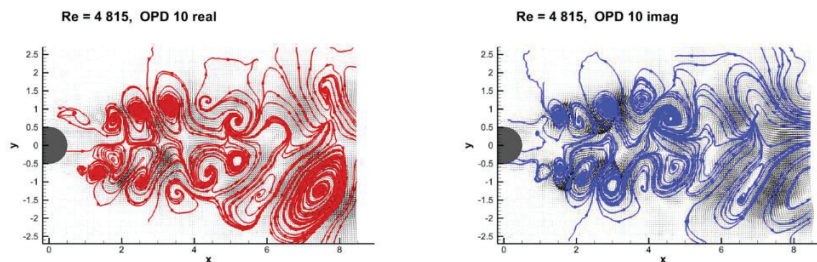


FIGURE 19. The OPD mode 10 topology, Reynolds number 4 815, real (left) and imaginary (right) parts.

The non-dominant higher order modes of the cases of different Reynolds numbers are of similar types and topologies as shown for the  $Re = 4\ 815$ , details could be different.

## CONCLUSIONS

The mean-time structure of the wake behind a circular cylinder has been shown for 4 different Reynolds numbers. Some tendencies in the wake topology, size and structure were demonstrated. However the presented experiment is to be considered as qualitative, as boundary conditions (the flow in jet) are not standard.

Dynamics of the wake exhibits systematical shift in the dominant frequency and evaluated Strouhal numbers. Typical frequency spectrum of dynamical structures in wake as well as their topologies were evaluated from time-resolved velocity distributions. The topologies and evolution of the typical dynamical structures presented in the wake are shown.

The results in the wake of a circular cylinder presented here could be compared with structures observed in the suction side of the inclined plate presented previously [5,8].

## ACKNOWLEDGMENT

This work was supported by the Grant Agency of the Czech Republic, project No. 17-01088S.

## REFERENCES

1. E. Achenbach and E. Heinecke On vortex shedding from smooth and rough cylinders in the range of Reynolds numbers  $6 \times 10^3$  to  $5 \times 10^6$ , *Journal of Fluid Mechanics*, Volume 109 (August 1981) pp. 239-251
2. R. D. Blevins, Flow Induced Vibration, 2nd Ed.. Van Nostrand Reinhold (1990)
3. J. H. Lienhard, Synopsis of Lift, Drag, and Vortex Frequency Data for Rigid Circular Cylinders, Washington State University, College of Engineering, *Bulletin* No. 300 (1966)
4. P. Procházka and V. Uruba, Reynolds Number Effect on Velocity Field and on Coherent Structures behind a Cylinder, AIP Conf. Proc. 2118, 030037-1–030037-4; (2019) 38th Meeting of Departments of Fluid Mechanics and Thermodynamics; Wellness and Kongress Hotel CHOPOK Liptovský Mikuláš; Slovakia; 19 June 2019 through 21 June 2019; Code 149090
5. P. Procházka, V. Uruba, V. Skála, Evolution of vortical structures behind an inclined flat plate, MATEC Web of Conferences 168 (2018) Article number 05003
6. A. Roshko, On the development of turbulent wakes from vortex streets. NACA Rep. 1191, pp.801-825 (1955)
7. V. Uruba, Near Wake Dynamics around a Vibrating Airfoil by Means of PIV and Oscillation Pattern Decomposition at Reynolds Number of 65 000, *Journal of Fluids and Structures*, 55, pp. 372-383 (2015)
8. V. Uruba, D. Pavlík, P. Procházka, V. Skála, V. Kopecký, On 3D flow-structures behind an inclined plate, EPJ Web of Conferences, 143, Article number 02137 (2017)
9. V. Uruba, Decomposition methods in turbulent research, EFM11, EPJ Web of Conferences, 25 01095 (2012)